

line when the absorption length is 1 m. A random magnetic field simulating this effect should not exceed $\sim 10^{-4}$ G in thallium and $\sim 10^{-3}$ G in lead. We shall conclude by pointing out that the precision achieved in the experiments on bismuth is quite sufficient to measure rotation angles $\sim 10^{-6}$ rad/m. Therefore, in a situation when the search for parity nonconservation in the strongly forbidden $M1$ $6p_{1/2} \rightarrow 7p_{1/2}$ transition in thallium is already under way,^[2] the proposed experimental detection of an optical activity of thallium vapor in the same frequency range seems realistic.

¹M. A. Bouchiat and L. Pottier, *Phys. Lett. B* **62**, 327 (1976).

²S. Chu, E. D. Commins, and R. Conti, *Phys. Lett. A* **60**, 96 (1977).

³L. L. Lewis, J. H. Hollister, D. C. Soreide, E. G. Lindahl, and E. N. Fortson, *Phys. Rev. Lett.* **39**, 795 (1977).

⁴P. E. G. Baird, M. W. S. M. Brimicombe, R. G. Hunt, G. J. Roberts, P. G. H. Sandars, and D. N. Stacey, *Phys. Rev. Lett.* **39**, 768 (1977).

⁵L. M. Barkov and M. S. Zolotarev, *Doklad na V Vsesoyuznoy Vavilovskoi konferentsii po nelineinoy optike* (Paper presented at Fifth All-Union Vavilov Conference on Nonlinear Optics), Novosibirsk, 1977.

⁶D. V. Neuffer and E. D. Commins, Preprint LBL 6043, 1977.

⁷V. N. Novikov, O. P. Sushkov, and I. B. Khriplovich, *Zh. Eksp. Teor. Fiz.* **71**, 1665 (1976) [*Sov. Phys. JETP* **44**, 872 (1976)].

⁸O. P. Sushkov, V. V. Flambaum, and I. B. Khriplovich, *Pis'ma Zh. Eksp. Teor. Fiz.* **24**, 502 (1976) [*JETP Lett.* **24**, 461 (1976)].

⁹V. N. Novikov, O. P. Sushkov, V. V. Flambaum, and I. B. Khriplovich, *Zh. Eksp. Teor. Fiz.* **73**, 802 (1977) [*Sov. Phys. JETP* **46**, 420 (1977)].

¹⁰R. Hultgren, R. L. Orr, P. D. Anderson, and K. K. Kelley, *Selected Values of the Thermodynamic Properties of the Elements*, American Society for Metals, Metals Park, Ohio (1973).

Translated by A. Tybulewicz

Optical resonators with periodic boundaries

V. M. Marchenko, T. M. Makviladze, A. M. Prokhorov, and M. E. Sarychev

P. N. Lebedev Physics Institute, USSR Academy of Sciences

(Submitted 1 July 1978)

Zh. Eksp. Teor. Fiz. **74**, 872-884 (March 1978)

Results are presented of theoretical and experimental investigations of optical resonators with periodic boundaries (ORPB). The natural oscillations for various periodic structures are obtained by solving a parabolic equation. It is shown that at definite resonator lengths there exist singular types of natural oscillations—periodic modes. The spatial distributions of the fields in the near and far zones are analyzed. Results are presented of an experimental investigation of a resonator with periodic modulation of the reflection coefficient in a neodymium-glass laser; these results are in satisfactory agreement with the theory. It is shown that ORPB make possible the shaping of extremely narrow directivity patterns.

PACS numbers: 42.60.Da

INTRODUCTION

Open optical resonators shape the spatial structure and the directivity pattern of laser radiation. The laser fields are natural modes of the resonator oscillations, and the configuration of these modes is determined by the resonator geometry. A resonator with plane-parallel mirrors^[1] has made it possible to obtain for the first time coherent emission in the optical band. The mode fields of stable resonators^[2,3] are concentrated in a limited volume, so that the diffractive divergence of the modes is determined by small apertures $2a \sim (\lambda L)^{1/2}$, where λ is the wavelength and L is the resonator length. This is why multimode lasing, which affects the directivity pattern adversely, takes place in lasers with large apertures.

From the energy point of view it is preferable to have large-volume laser media, so that an important problem is to generate oscillation modes whose fields occupy

the entire exit aperture. From this point of view, definite advantages are offered by unstable resonators^[4] such as the telescopic one.^[5]

A new interesting possibility is uncovered by optical resonators in which at least one of the mirrors is a two-dimensional grid with periodically varying reflection coefficient. The first results of the investigation of such resonators were reported recently.^[6] It was shown that these resonators ensure good filling of the active medium, and the divergences of the individual light spots in the far zone can reach the diffraction value over the total aperture of the reticular mirror. These features of such systems were not noted in earlier experiments.^[7-9]

It was indicated^[8,9] that the theoretical investigation of diffraction resonators is a complex task. This is apparently the reason why these resonators were treated in some papers by simplified methods.^[10,11] One study^[12] enhanced the interest in the study of such sys-

tems, but provided no satisfactory theoretical analysis.

We present here the results of a theoretical and experimental investigation of open optical resonators with periodic boundaries (ORPB). On the basis of the solution of the boundary-value problem of the equations of electrodynamics, we investigate the natural modes of the ORPB oscillations, and calculate the fields inside and outside the resonator for different periodic structures. The conditions for the excitation of various ORPB modes are investigated experimentally and interpreted. It is shown that the angular divergence of individual lobes of the directivity pattern is close to the diffraction value at the exit aperture, and a method of controlling the radiation divergence is demonstrated.

A. THEORY

1. Fundamental relations

Consider a system consisting of two infinite plane mirrors whose surfaces are defined by the relations $z = \pm l$, $-\infty < x, y < +\infty$. Let one of the mirrors (at $z = -l$) have an amplitude reflection coefficient $T_1 = 1 - \beta_1$ that is independent of the coordinates, and let the second have a coefficient $T_2(x, y)$ that depends on x and y . We assume the mirrors to be thin enough to be able to neglect the changes that take place in the fields as they propagate inside the mirrors. Taking the time dependence of the fields in the form $\exp(-i\omega t)$, where $\omega = ck$ (k is the wave number), we start with the scalar wave equation for any component W of the electromagnetic field. This equation, by virtue of the condition $(\text{Re}k)l \gg 1$, reduces to a parabolic form whose solution is best represented in the form^[3]

$$W(\xi, \eta, \zeta) = \Phi_1(\xi, \eta, \zeta) \exp(2ikl\zeta) - (-1)^q \Phi_2(\xi, \eta, -\zeta) \exp(-2ikl\zeta), \\ \xi = (k/2l)^{1/2}x, \quad \eta = (k/2l)^{1/2}y, \quad \zeta = z/2l,$$

where $\Phi_1(\xi, \eta, \zeta)$ determines the field of the wave incident on the mirror $z = l$, $\Phi_2(\xi, \eta, -\zeta)$ is the diffraction field produced by the mirror, and q is an integer. The boundary conditions for the transverse components of the electric field are of the form

$$\Phi_1(\xi, \eta, -1/2) = \exp(i\chi) T_1 \Phi_2(\xi, \eta, 1/2), \\ \Phi_2(\xi, \eta, -1/2) = \exp(i\chi) T_2(\xi, \eta) \Phi_1(\xi, \eta, 1/2), \quad (1)$$

where $\chi = 2kl - \pi q$. Relations (1) correspond to the boundary conditions on the surface of dielectric at small wave incidence angles. For a factorizable reflection coefficient $T_2(\xi, \eta) = T_2^q(\xi) T_2^b(\eta)$, the three-dimensional problem reduces to a two-dimensional one^[1,3] if we put

$$\Phi_i = \Phi_i^a(\xi, \zeta) \Phi_i^b(\eta, \zeta), \quad i=1, 2.$$

We shall therefore consider henceforth the equations

$$\frac{\partial^2 \Phi_i(\xi, \zeta)}{\partial \xi^2} + 2i \frac{\partial \Phi_i(\xi, \zeta)}{\partial \zeta} = 0, \quad (2)$$

with the boundary conditions

$$\Phi_1(\xi, -1/2) = \exp(i\chi) T_1 \Phi_2(\xi, 1/2), \\ \Phi_2(\xi, -1/2) = \exp(i\chi) T_2(\xi) \Phi_1(\xi, 1/2).$$

and

$$W(\xi, \zeta) = \Phi_1(\xi, \zeta) \exp(2ikl\zeta) - (-1)^q \Phi_2(\xi, -\zeta) \exp(-2ikl\zeta).$$

It is easy to obtain the integral equations

$$f_1(\xi) = \exp(2i\chi) T_1 \int_{-\infty}^{\infty} K_1(\xi, \xi') f_1(\xi') d\xi', \quad (3)$$

$$f_2(\xi) = \exp(2i\chi) T_2 T_1(\xi) \int_{-\infty}^{\infty} K_2(\xi, \xi') f_2(\xi') d\xi', \quad (4)$$

which determine the incident and reflected fields at $z = -l$:

$$f_1(\xi) = \Phi_1(\xi, -1/2), \quad f_2(\xi) = \Phi_2(\xi, -1/2).$$

The kernels of (3) and (4) are

$$K_1(\xi, \xi') = \int_{-\infty}^{\infty} \Gamma(\xi - \xi'', 1) T_2(\xi'') \Gamma(\xi'' - \xi', 1) d\xi'', \\ K_2(\xi, \xi') = \int_{-\infty}^{\infty} \Gamma(\xi - \xi'', 1) \Gamma(\xi'' - \xi', 1) d\xi'',$$

where $\Gamma(\xi - \xi', \zeta - \zeta')$ is the Green's function of Eq. (2), and the values of χ should be determined as the eigenvalues of Eqs. (3) and (4) and yield the frequency spectrum of the natural oscillations of the resonator.

2. ORPB with sinusoidal reflection coefficient

We consider the solution of Eqs. (3) and (4) for a sinusoidal grid

$$T_2(\xi) = 1 - \beta_2(1 + m \cos \alpha \xi), \quad \alpha = (2\pi/p)(2l/k)^{1/2}, \quad (5)$$

where p is the period of the grid, $0 \leq \beta_2 \leq 1/2$, $0 \leq m \leq 1$. We seek the solution of (4) in the form

$$f_2(\xi) = \exp(is_j \xi) \sum_{n=-\infty}^{\infty} A_n(\alpha) \exp(in\alpha \xi).$$

Then

$$1/2(1 - \beta_2) \beta_2 m A_{n-1} \exp[2i\alpha^2 n - i(\alpha^2 - 2\alpha s_j)] - A_n \{(1 - \beta_2)(1 - \beta_2) \\ - \exp[i(s_j + n\alpha)^2 - i\eta]\} + 1/2(1 - \beta_2) \beta_2 m A_{n+1} \exp[-2i\alpha^2 n \\ - i(\alpha^2 + 2\alpha s_j)] = 0, \quad \eta = 2\chi. \quad (6)$$

The roots of the equation $\det\{A\} = 0$ (where $\{A\}$ is the matrix of the coefficients A_n of the system (6)) determine the function $\bar{\chi} = \bar{\chi}(\alpha, s_j)$, i.e., the natural frequencies of the ORPB.

At $\beta_2 = 0$ we obtain $A_n = 0$ ($n \neq 0$) and

$$\bar{\chi} = \eta_0 = s_j^2 - 4\pi j + i \ln(1 - \beta_1), \quad j = 0, \pm 1, \dots, \quad (7a)$$

where s_j is an arbitrary real number and $f_2(\xi)$ takes the form of a traveling or standing wave^[3]:

$$f_2^{(0)}(\xi) = \exp(is_j \xi), \quad f_2^{(j)}(\xi) = \cos(s_j \xi), \quad f_2^{(k)}(\xi) = \sin(s_j \xi). \quad (7b)$$

Since $\beta_2 \leq 1/2$, the solution of (4) can be obtained by perturbation theory in β_2 :

$$f_2(\xi) = f_2^{(0)}(\xi) + \beta_2 f_2^{(1)}(\xi) + \beta_2^2 f_2^{(2)}(\xi) + \dots, \quad \bar{\chi} = \bar{\chi}_0 + \beta_2 \mu_1 + \beta_2^2 \mu_2 + \dots \quad (8)$$

Choosing $f_2^{(0)}(\xi) = \cos(s_j \xi)$, we obtain

$$f_2^{(1)}(\xi) = A_1^{(1)} \cos(\alpha + s_j) \xi + A_1^{(1)} \cos(\alpha - s_j) \xi, \quad \mu_1 = -i/2,$$

where

$$A_{\pm 1}^{(1)} = -1/2 m \{1 - \exp[-i(\alpha^2 \pm 2\alpha s_j)]\}^{-1}.$$

A similar structure is possessed by the functions $f_2^{(n)}(\xi)$ obtained in higher orders of perturbation theory.^[13]

The solution of (3) is obtained in similar fashion. The existence of the solution (8) demonstrates that in the region where perturbation theory is valid natural oscillations can arise in the system at all values of λ , p , and $L = 2l$. They are the solutions (7) for a resonator with an ideally reflecting mirror at $z = l$ plus increments due to the periodic modulation of $T_2(\xi)$.

The structure of the coefficients of the expansion of $f_2^{(n)}$ in terms of $\cos(s_j \pm n\alpha)\xi$ shows that in the vicinities of the values of α and s_j determined from the equations

$$\alpha^2 + 2\alpha s_j = 2\pi n_1, \quad \alpha^2 - 2\alpha s_j = 2\pi n_2, \quad n_{1,2} = 0, \pm 1, \pm 2, \dots \quad (9)$$

perturbation theory ceases to hold. We note that by virtue of the condition $(\text{Re}k)l \gg 1$ all the quantities in (9) can be regarded as real. From (9) we have

$$\alpha^2 = \pi(n_1 + n_2), \quad s_j^2 = s_{j,n_1}^2 = \pi(n_1 - n_2)^2/4(n_1 + n_2) \quad (n_1 > -n_2). \quad (10)$$

If a value of α^2 satisfying the first condition of (10) is specified, only one of the numbers n_1 and n_2 can be arbitrary. The corresponding values of s_j will henceforth be numbered by the index n_1 . We present expressions for the fields when (9) are satisfied. Two cases are possible here:

a) $n_1 + n_2$ is odd. then

$$\alpha^2 = \pi(2r+1), \quad s_{j,n_1}^2 = \pi[2(n_1 - r) - 1]^2/4(2r+1)$$

(r is an integer) and

$$W(\xi, \zeta) = C_1 \sum_{n=-\infty}^{\infty} \exp[-i(s_{j,n_1} + 2n\alpha)\zeta/4] \cos(s_{j,n_1} + 2n\alpha)\xi \\ \times \left\{ \left(\frac{1-\beta_1}{1-\beta_2} \right)^{1/2} \exp[-1/2 \zeta \ln(1-\beta_1)(1-\beta_2)] \right. \\ \times \exp[-i\pi(2j-q+2nn_1+n(2n-1)(2r+1)\zeta)] \\ \left. - (-1)^{r+n} \exp[1/2 \zeta \ln(1-\beta_1)(1-\beta_2)] \right. \\ \left. \times \exp[i\pi(2j-q)+2nn_1+n(2n-1)(2r+1)\zeta] \right\}, \quad (11)$$

where C_1 is an arbitrary constant.

b) $n_1 + n_2$ is even. Then

$$\alpha^2 = 2\pi r, \quad s_{j,n_1}^2 = \pi(n_1 - r)^2/2r$$

and the field in the near zone of the mirror $\zeta = 1/2$ is of the form

$$W\left(\xi, \frac{1}{2}\right) = \frac{\beta_2(1-\beta_1)^{1/2}}{(1-\beta_2)^{1/2}} \exp\left[-\frac{i}{4}(s_{j,n_1}^2 - 2\pi q')\right] \\ \times \cos(s_{j,n_1}\xi) \left\{ C_1 \sum_{n=-\infty}^{\infty} (-1)^n \cos 2n\alpha\xi + 2iC_2 \sum_{n=1}^{\infty} (-1)^{n-1} \sin(2n-1)\alpha\xi \right\}, \\ q' = q - 2j;$$

C_1 and C_2 are arbitrary constants. The frequency spectrum in both cases is determined by the relation

$$\chi = s_{j,n_1}^2 - 4\pi j + i \ln(1-\beta_1)(1-\beta_2). \quad (12)$$

The structure of the fields in the near zone becomes clear if the following representation is used: in case a)

$$W\left(\xi, \frac{1}{2}\right) = C_1 \frac{\pi\beta_2(1-\beta_1)^{1/2}}{\alpha(1-\beta_2)^{1/2}} \exp\left[-\frac{i}{4}(s_{j,n_1}^2 - 2\pi q')\right] \\ \times \cos(s_{j,n_1}\xi) \sum_{n=-\infty}^{\infty} \delta\left[\xi - (2n-1)\frac{\pi}{2\alpha}\right], \quad (13)$$

in case b)

$$W\left(\xi, \frac{1}{2}\right) = \frac{\pi\beta_2(1-\beta_1)^{1/2}}{\alpha(1-\beta_2)^{1/2}} \exp\left[-\frac{i}{4}(s_{j,n_1}^2 - 2\pi q')\right] \\ \times \cos(s_{j,n_1}\xi) \sum_{n=-\infty}^{\infty} [C_1 + i(-1)^n C_2] \delta\left[\xi - (2n-1)\frac{\pi}{2\alpha}\right]. \quad (14)$$

It follows from (13) and (14) that the field in the near zone of the boundary $\zeta = 1/2$ has maxima at the points of inflection of the reflection coefficient (5). It is easy to show that the field in the near zone of the mirror $\zeta = -1/2$ has the same structure, but in case a) its maxima are shifted by $p/4$ relative to the maxima at $\zeta = 1/2$.

We consider in greater detail the conditions (9). It follows from them that

$$L = 2l = (p^2/2\lambda)(n_1 + n_2).$$

Thus, in an ORPB with given L natural oscillations of the type (13) and (14) are possible with wavelengths that are multiples of $p^2/2L$. At other wavelengths, oscillations of this type are impossible, and the natural fields are determined in accordance with (8).

In the cases considered above, a) $n_1 + n_2 = 2r + 1$ and b) $n_1 + n_2 = 2r$, the distances L are respectively

$$L_1 = L_0(2r-1)/4, \quad L_2 = L_0 r/2 \quad (L_0 = 2p^2/\lambda, \quad r = 1, 2, \dots).$$

It should be noted that, as first shown by Rayleigh (see, e.g.,^[14]), at distances equal to an integer L_0 an image is produced of a passive diffraction grating of infinite length irradiated by a plane wave. Thus, the singular resonator properties in the cases $L = L_{1,2}$ are due to the reproduction of the wave front on the boundaries. This agrees with the resonator-system treatment presented in^[2].

According to (9) and (12)

$$k = \frac{\pi}{2l} q' + \frac{1}{4l} s_{j,n_1}^2 + \frac{i}{4l} \ln(1-\beta_1)(1-\beta_2). \quad (15)$$

By virtue of $(\text{Re}k)l \gg 1$, at any β_2 , the imaginary part of k is negligibly small compared with the real one. It follows from (11) that these solutions can be regarded as fields having the following wave-vector z component

$$k_z = \frac{\pi}{2l} q' + \frac{i}{4l} \ln(1-\beta_1)(1-\beta_2)$$

and the x component $k_x = s_{j,n_1}(k/2l)^{1/2}$. The fields (13)

and (14) can be treated as waves propagating with "quasimomentum" k_x over discrete "nodes" $x_n = p(2n-1)/4$. In particular, at $s_{j,n_1} = 0$ the oscillations in these "nodes" are in phase. Expression (15) can now be represented in the form $k = k_x + k_x^2/2k$, i.e., as an expansion of $k = (k_x^2 + k_p^2)^{1/2}$ in the small parameter $|k_x/k_p|$. The indicated representation is therefore valid at $s_{j,n_1}^2 \ll \pi q'$, with $q' \gg 1$, since $(\text{Re}k)l \approx |k|l \gg 1$. This agrees with the introduction of a dielectric-surface reflection coefficient that does not depend on ϑ . The possible natural modes (13) and (14) must be identified by two integers q' and n_1 . Their quality factors are

$$Q_{q'} = -\pi q' / \ln(1-\beta_1)(1-\beta_2).$$

3. ORPB with steplike reflection coefficient

Let

$$T_2(\xi) = 1 - \beta_2 + \beta_2 \Pi(\xi), \quad 0 \leq \beta_2 < 1, \quad (16)$$

where

$$\Pi(\xi) = \begin{cases} 0, & \text{if } |\xi - n\bar{p}| \leq \bar{\tau}/2, \quad n=0, \pm 1, \dots, \\ \gamma, & \text{if } \bar{\tau}/2 < \xi - n\bar{p} < \bar{p} - \bar{\tau}/2, \end{cases}$$

$\bar{p} = p(k/2l)^{1/2}$ is the dimensionless period, $\bar{\tau} = \tau(k/2l)^{1/2}$, and $\sigma = (p - \tau)/\tau$ is the porosity of the grid. By writing down the solutions of (3) and (4) in the form of a series in powers of β_2 , in analogy with (8), we can show that under conditions (9) the natural oscillations cease to be determined by this series.

We consider next oscillations that set in when relations (9) are satisfied. It can be shown^[13] that in this case the eigenvalues $\bar{\chi}$ are determined by expressions (12). The possible types of natural oscillations, frequency, and Q are determined from formula (15), in which it is necessary to change the interval of the possible values of β_2 , namely $0 \leq \beta_2 < 1$. The expression for the field on a periodic boundary is of the form

$$W\left(\xi, \frac{1}{2}\right) = A \frac{\beta_2(1-\beta_1)^{1/4}}{(1-\beta_2)^{3/4}} \exp\left[-\frac{i}{4}(s_{j,n_1}^2 - 2\pi q')\right] \cos(s_{j,n_1}\xi) G(\xi), \quad (17a)$$

where

$$G(\xi) = \begin{cases} g(\xi), & \text{if } |\xi - n\bar{p}| \leq \bar{\tau}/2, \\ 0, & \text{if } \bar{\tau}/2 < \xi - n\bar{p} < \bar{p} - \bar{\tau}/2, \end{cases} \quad (18)$$

$g(\xi)$ is an arbitrary function. The behavior of the periodic (with period \bar{p}) amplitude part of the field on the mirror $\xi = 1/2$ depends on the value of s_{j,n_1} :

$$W\left(\xi, -\frac{1}{2}\right) = -\frac{A\beta_1 \exp[-i(s_{j,n_1}^2 + 2\pi q')/4]}{[(1-\beta_1)(1-\beta_2)]^{1/4}} \times \cos(s_{j,n_1}\xi) \cdot \begin{cases} G(\xi), & n_1 \text{ even} \\ G(\xi + \pi/\alpha), & n_1 \text{ odd} \end{cases} \quad (17b)$$

It is important that the solutions (17) exist only if $n_1 + n_2$ is even.

$$L = L_2 = L_0 r/2, \quad s_{j,n_1}^2 = \pi(n_1 - r)^2/2r. \quad (19)$$

It should be noted that expression (18) gives only the general structure of the function $G(\xi)$, but not its concrete form. The obtained natural oscillation of an ORPB with $L = L_2$, corresponding to fixed indices n_1 and q' , can have a different dependence on the transverse coordinate ξ . The concrete form of such a mode can be determined by the conditions for the excitation of the ORPB.

It is seen from (17) that the fields in the near zone of a periodic mirror differ from zero in those places ("holes") where $T_2(\xi)$ has minima, and conversely are equal to zero on those section where $T_2(\xi)$ is maximal. It is easy to show that there exist natural oscillations with opposite field structure in the near zone:

$$\Pi\left(\xi, \frac{1}{2}\right) = \frac{A\beta_2(1-\beta_1)^{1/4}}{(1-\beta_2)^{3/4}} \exp\left[-\frac{i}{4}(s_{j,n_1}^2 - 2\pi q')\right] \cos(s_{j,n_1}\xi) \bar{G}(\xi), \quad (20a)$$

$$\Pi\left(\xi, -\frac{1}{2}\right) = -\frac{A\beta_1}{[(1-\beta_1)(1-\beta_2)]^{1/4}} \exp\left[-\frac{i}{4}(s_{j,n_1}^2 + 2\pi q')\right] \times \cos(s_{j,n_1}\xi) \cdot \begin{cases} \bar{G}(\xi), & n_1 \text{ even} \\ \bar{G}(\xi + \pi/\alpha), & n_1 \text{ odd} \end{cases} \quad (20b)$$

Here

$$\beta_2 = \beta_2(1-\gamma), \quad (n_1 + n_2) \text{ even}, \\ \bar{G}(\xi) = \begin{cases} 0, & \text{if } |\xi - n\bar{p}| \leq \bar{\tau}/2, \\ \bar{g}(\xi), & \text{if } \bar{\tau}/2 < \xi - n\bar{p} < \bar{p} - \bar{\tau}/2. \end{cases}$$

and the eigenvalues $\bar{\chi}$ are given by

$$\bar{\chi} = s_{j,n_1}^2 - 4\pi j + i \ln(1-\beta_1)(1-\beta_2 + \beta_2\gamma).$$

On the mirror $z = -l$ the distributions of the fields with odd n_1 are displaced by $p/2$ relative to the distributions of the fields with even n_1 ; there is no such displacement on the periodic mirror. The maxima of the intensity on the periodic mirrors occur in the sections with large values of the reflection coefficient. The quality factors of the natural oscillations (20)

$$\bar{Q}_{q'} = -\pi q' / \ln(1-\beta_1)(1-\beta_2 + \beta_2\gamma)$$

exceed those of the oscillations (17). The modes (17) and (20) will hereafter be called periodic modes.

The general case of ORPB with arbitrary periodic $T_2(\xi)$ is considered in^[13].

To treat the three-dimensional case it suffices to note that if $T_2(x)$ and $T_2(y)$ are defined by the same relation of the form (16), then at $L = L_2$ a complete identification of the modes calls for the specification of three numbers q' , n_1 , and m_1 , with $k_y = s_{j,m_1}(k/2l)^{1/2}$, where

$$s_{j,m_1}^2 = \pi(m_1 - m_2)^2/4(m_1 + m_2), \quad m_2 = 2\lambda L/p^2 - m_1(m_1 + m_2 = n_1 + n_2).$$

If the periods $T_2(x)$ and $T_2(y)$ are different and equal to p_x and p_y , then the system has periodic modes at $L = p_x^2(n_1 + n_2)/2\lambda$, and $n_1 + n_2 = (p_y/p_x)^2(m_1 + m_2)$, where $m_1 + m_2$ is even.

It should be noted that the method of treating the ORPB as a natural-mode problem is approximate.^[3]

The method is more accurate the larger the Q of the oscillations. The approximation manifests itself mathematically in that the fact that k is imaginary is neglected in the conditions (9).

4. Field in far zone

If the wave front at $z=l$ is bounded by an aperture $|x| \leq a$, then the in the far zone is determined in the Fraunhofer approximation by the usual formula

$$F(x, z) = -\frac{i}{\lambda z} \exp\left(i \frac{2\pi}{\lambda} z\right) \int_{-a}^a W(x_1, l) \exp\left(-i \frac{2\pi}{\lambda z} x x_1\right) dx_1 \exp\left(i \frac{\pi x^2}{\lambda z}\right), \quad (21)$$

where $W(x_1, l)$ is the field in the near zone. Expression (21) describes the diffraction picture at $y=0$. The two-dimensional picture in the case of a one-dimensional grid $T_2(x, y) = T_2(x)$ is obtained by multiplying (21) by $\text{sinc}(by/\lambda z)$, where $\text{sinc} u = \sin(\pi u)/\pi u$ and $(-b, b)$ is the width of the aperture along the y axis. In the case of a two-dimensional grid, the total diffraction picture is obtained by multiplying (21) by

$$F(y, z) = \exp\left(i \frac{\pi}{\lambda z} y^2\right) \int_{-b}^b W(y_1, l) \exp\left(-\frac{2\pi}{\lambda z} y y_1\right) dy_1,$$

where $W(y, l)$ is the field in the near zone, obtained by solving the two-dimensional problem with $T_2 = T_2(y)$. Bearing in mind this transition to the three-dimensional case, we confine ourselves below to calculation of the diffraction field at $y=0$.

In the case of a sinusoidal coefficient (5), the principal intensity maxima are of equal height and are located at the angles

$$\theta_n = \left[\frac{4\pi}{p} n \pm s_{j,n} \left(\frac{\pi}{\lambda l} \right)^{1/2} \right] \frac{\lambda}{2\pi}.$$

Consider the case of an ORPB with a steplike reflection coefficient (16) upon excitation of the periodic mode (20). Assuming for the sake of argument that $G(x)$ is an even function,

$$\bar{G}(x) = \sum_{n=0}^{\infty} b_n \cos(2\pi n x/p),$$

we obtain for the radiation intensity $I = |F(x, z)|^2$ under the condition $p \ll a$

$$I = \frac{\bar{A}^2 \beta_2^2 (1-\beta_1)^{1/2} a^2}{(1-\beta_2)^{1/2} \lambda^2 z^2} \sum_{n=-\infty}^{\infty} b_n'^2 \left\{ \text{sinc}^2 \left[\left(s_{j,n} \left(\frac{\pi}{\lambda l} \right)^{1/2} - \frac{2\pi x}{\lambda z} + \frac{2\pi}{p} n \right) \frac{a}{\pi} \right] \right. \\ \left. \text{sinc}^2 \left[\left(-s_{j,n} \left(\frac{\pi}{\lambda l} \right)^{1/2} - \frac{2\pi x}{\lambda z} + \frac{2\pi}{p} n \right) \frac{a}{\pi} \right] \right\}, \quad b_0' = 2b_0, \quad b_n' = b_n \quad (n \neq 0). \quad (22)$$

The diffraction pattern constitutes a consequence of intensity maxima fanning out in the directions

$$\theta_n = \left[\frac{2\pi}{p} n \pm s_{j,n} \left(\frac{\pi}{\lambda l} \right)^{1/2} \right] \frac{\lambda}{2\pi}.$$

The angle between the neighboring maxima is λ/p , and their width, determined from the first zeroes of $\text{sinc} u$, equals $\delta\theta = \lambda/a$. The dependence of the relative intensity

$$\bar{I} = \frac{z^2 \lambda^2 (1-\beta_2)^{1/2}}{\bar{A}^2 \beta_2^2 a^2 (1-\beta_1)^{1/2}} I$$

on $\bar{x} = px/\lambda z$ is a function that has sharp maxima at

$$\bar{x}_n = n + ps_{j,n} (\pi \lambda l)^{-1/2},$$

and its values at $\bar{x} = \bar{x}_n$ are $b_n'^2$, i.e., $b_n'^2$ is the envelope of these maxima. Since $\lim_{n \rightarrow \infty} b_n' = 0$, the envelope distinguishes a certain number of maxima n^* near the zeroth one. The extent to which this distinction is effective depends on p , σ , and the concrete form of $\bar{g}(x)$. It is easily seen that the narrowest radiation corresponds to excitation of a periodic mode $\bar{g}(x) = \text{const}$, when b_n is determined by the porosity of the grid:

$$b_0 = \frac{\sigma}{1+\sigma}, \quad b_n = \frac{2}{1+\sigma} \text{sinc} \frac{n}{1+\sigma} \quad (n \neq 0). \quad (23)$$

It can be assumed that $b_n/b_0 < 1$ at $|n\sigma/(1+\sigma)| \geq 1$, i.e., for $|n| \geq [1+\sigma^{-1}]$ (the symbol $[...]$ denotes the integer part of the number). Thus, $n^* = 2[1+\sigma^{-1}] - 1$ if $1+\sigma^{-1} - [1+\sigma^{-1}] \ll 1$ and $n^* = 2[1+\sigma^{-1}] + 1$ if $1+\sigma^{-1} - [1+\sigma^{-1}]$ is not too small. The number $n^* = 1$ at $\sigma \gg 1$, and the effective angular divergence $\delta\theta$ of the radiation is determined by the diffraction on the aperture: $\delta\theta \sim \lambda/a$; the directivity pattern of the ORPB radiation consists of a single narrow lobe.

B. EXPERIMENT

1. Field in near zone

The excitation of the ORPB was investigated experimentally with the aid of a neodymium-glass laser. The ORPB was made up of two flat dielectric mirrors, one solid and the other reticular. The two-dimensional reticular mirrors with porosity $\sigma=1$ were prepared by vacuum sputtering on a glass substrate through masks produced by photolithography. The mirror reflection coefficients ranged from 0.7 to 0.99. The characteristic distances between the mirrors, L_R , which satisfy the condition for the reproduction of the field on the mirror grid, are given by the formula

$$L_n = L_2 + l'(1-1/n'), \quad (24)$$

where L_2 is given by (19) and the second term takes into account the change introduced in the optical path by the rod of length l' and refractive index n' . At $\lambda = 1.06 \mu\text{m}$, $p = 1 \text{ mm}$, $l' = 320 \text{ mm}$, $n' = 1.52$ and $r = 1$ we have $L_R = 105 \text{ cm}$.

The distribution of the laser-intensity distribution in the near and far zones was investigated by the method of burning through the target (see Figs. 1, 2, 5, and 6) and by a photographic method (Fig. 4).

The experimental criterion for the excitation of periodic modes was assumed to be the appearance of lasing with a characteristic periodic distribution of the radiation intensity in the near zone of the reticular and solid mirrors (see, e.g., Figs. 1 (1 and 2)). The directions of the x and y axes of the resonator are shown above the figures).

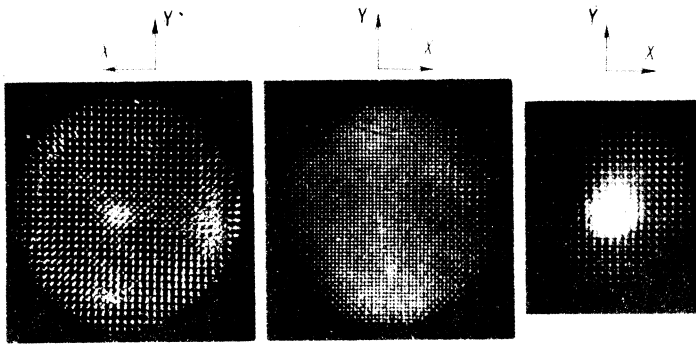


FIG. 1. Distribution of the emission intensity of a laser with ORPB in the near zone of a reticular (1) and solid (2) mirrors and in the far zone (3) of the focal plane of an objective with focal length 1 m. The linear scale on frames 1, 2, and 3 is the same. The grid period is 1 mm.

Given the distance L_R between the mirrors, the intensity distribution in the near zone of the reticular mirror is a replica of the mirror grid. This corresponds to excitation of modes (20) with high Q and with fields localized on the mirror meshes. The form of the distribution depends little on the parallelism of the mirrors.

The intensity distribution in the near zone of the solid

mirror, when the mirrors are adjusted to be parallel with accuracy better than $10''$, usually takes the form of grids with period p , shifted relative to each other by $p/2$ along the coordinates x or y , or along both x and y , i.e., in a diagonal direction (Fig. 1 and 2). This intensity distribution agrees with expression (20b) for fields on a solid mirror. To identify the modes it is convenient to introduce next the transverse indices $n_0 = n_1 - 1$ and $m_0 = m_1 - 1$. Then Fig. 1 (2) illustrates excitation of modes with all possible combinations of n_0 and m_0 in parity. Misalignment of the mirrors by an amount up to $30''$ leads to an appreciable change of the intensity distribution in the near zone of the solid mirror (Fig. 2).



FIG. 2. Influence of misalignment of mirrors on the distribution of the intensity of a laser with ORPB in the far zone of a solid mirror (1,1), (1,2), (1,3) and in the far zone (2,1), (2,2), (2,3). The scale is the same as in Fig. 1. The first index in the parentheses numbers the frame along the x axis, and the second along the y axis.

Figure 2 (1,1) (the first and second indices in the parentheses denote the numbers of the frames in the x and y directions) demonstrates the excitation of modes that are even-even and odd-odd in n_0 and m_0 . The intensity distributions of these modes take the form of grids shifted relative to each other along the x and y axes. The intensity distribution of the odd-odd modes (Fig. 2 (1,2)) is a single grid shifted by $p/2$ along x and y relative to the reticular mirror. It is seen from Fig. 2 (1,3) that the intensity distribution of the even-odd and odd-even modes are shifted by $p/2$ respectively relative to the distribution of the odd-odd modes.

The experiments have shown that the least sensitive to misalignment are the odd-odd modes. The intensity distribution in the near zone was independent of the mirror reflection coefficient.

2. Field in far zone

The directivity pattern of a laser with ORPB was investigated by determining the distribution of the intensity in the far zone—in the focal plane of a lens with focal length 1m. The intensity distribution at all pump levels, starting with the threshold value, has a multi-lobe character, as seen from all the drawings.

It follows from (22), the angular spectrum of an individual modes depends on the concrete form of $\bar{g}(x)$. In the particular case of constant $\bar{g}(x)$, the one-dimensional angular spectrum, according to (22) and (23), is

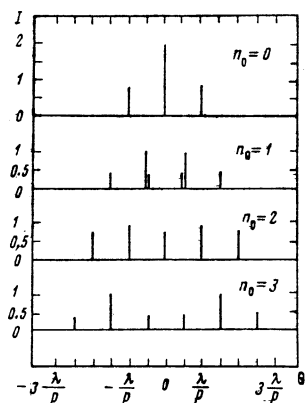


FIG. 3. Angle spectrum of the relative intensity I of the ORPB modes with $n_0 = 0$ to 3 at the porosity of reticular mirror 1. The separation of the harmonics of mode $n_0 = 1$ is shown only for illustration.

given by the following expression for the relative intensity:

$$\begin{aligned}
 I = & 2 \operatorname{sinc}^2 \left[\left(s_{j,n_1} \left(\frac{\pi}{\lambda L} \right)^{1/2} - \frac{2\pi x}{\lambda z} \right) \frac{a}{\pi} \right] \\
 & + \operatorname{sinc}^2 \left[\left(s_{j,n_1} \left(\frac{\pi}{\lambda L} \right)^{1/2} + \frac{2\pi x}{\lambda z} \right) \frac{a}{\pi} \right] \\
 & + \sum_{n=-\infty}^{\infty} \operatorname{sinc}^2 \left(\frac{n}{2} \right) \left\{ \operatorname{sinc}^2 \left[\left(s_{j,n_1} \left(\frac{\pi}{\lambda L} \right)^{1/2} - \frac{2\pi x}{\lambda z} + \frac{2\pi}{p} n \right) \frac{a}{\pi} \right] \right. \\
 & \left. + \operatorname{sinc}^2 \left[\left(-s_{j,n_1} \left(\frac{\pi}{\lambda L} \right)^{1/2} - \frac{2\pi x}{\lambda z} + \frac{2\pi}{p} n \right) \frac{a}{\pi} \right] \right\}, \quad (25)
 \end{aligned}$$

where the prime at the summation sign means $n \neq 0$. For $n_0 = 0$ to 3, the main components of the angle spectrum are shown in Fig. 3 (the splitting at $\theta = \pm \lambda/p$ for the mode $n_0 = 1$ is shown only for illustration, and the intensity is equal to the sum of the split components).

The experimentally observed two-dimensional angle spectrum is discrete, and the smallest angles between the lobes along the x and y axes are equal to $\lambda/2p$, corresponding to excitation of modes with all possible combinations of transverse indices n_0 and m_0 , and agrees with Eq. (25)—see Fig. 1(3) and Fig. 3.

The angle spectrum depends on the departure of the mirrors from parallelism and correlates with the intensity distribution in the near zone of the reticular mirror (Fig. 2). The angle spectrum constitutes two-dimensional grids. As seen from Fig. 2 (2, 1) and Fig. 2

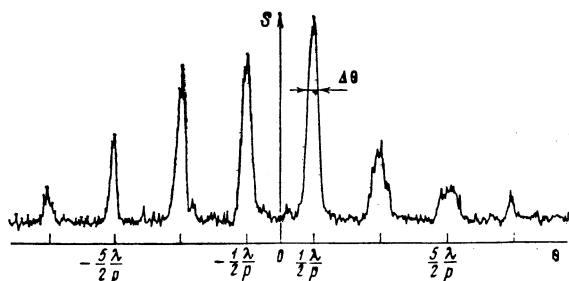


FIG. 4. Microphotogram of the distribution of the emission intensity of a laser with ORPB in the far zone along the x axis following excitation of odd-odd modes ($\Delta\theta$ is the angle width of the emission lobe at half-intensity level).

(2, 2), the excited even-even modes have a central lobe directed along the z axis, as well as side lobes, separated from the central one by angles that are multiples of λ/p (see Fig. 3, $n_0 = 0, 2$). The lobes of the odd-odd modes are also separated by λ/p from one another and are inclined by an angle $\lambda/2p$ to the lobes of the even-even modes (cf. Fig. 3, $n_0 = 0, 2$ and $n_0 = 1, 3$). The lobes of the even-odd and odd-even modes are inclined at an angle $\lambda/2p$ to the lobes of the odd-odd modes (Fig. 2 (2.4)).

It follows from (22) that the angular divergence of the mode lobes should be determined by the exit aperture on which the lasing takes place. Figure 4 shows a one-dimensional microphotogram of the emission intensity in the far zone of odd-odd modes at a near-threshold pump level. The asymmetry of the lobe intensity relative to the resonator axis is apparently due to inclination of the mirrors. Photometry of individual spots in the far zone shows that the obtained lobe divergence exceeds the diffraction value by several times.

The divergence of the mode lobes increases with increasing pump, but not as rapidly as the divergence of the modes of a resonator with solid mirrors. Figure 5 shows the case when the mirror grid was deposited only on the central part of the substrate. The first to be excited are periodic modes, and the characteristic periodic distribution of the intensity in the near zone

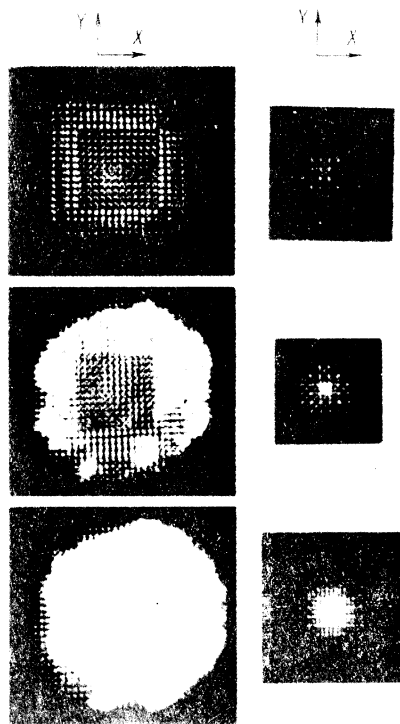


FIG. 5. Emission intensity distribution versus pump of a laser with ORPB having a transverse dimension equal to one-third the diameter of the exit aperture, in the near zone of the reticular mirror (1, 1), (1, 2), (1, 3) and in the far zone (2, 1), (2, 2), (2, 3). The upper frames correspond to 8% above threshold, the middle ones to 15%, and the lower to 35%. The scale and notation are the same as in Fig. 2.

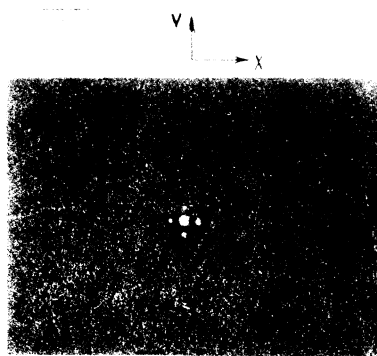


FIG. 6. Distribution of emission intensity of laser with ORPB in the far zone. Porosity of reticular mirror 50. The scale is magnified 1.8 times compared with Fig. 2.

extends beyond the grid. It is determined apparently by the field of the diffraction losses of the periodic modes, which is enhanced in the resonator. With increasing pump, lasing of the modes of the resonator with solid mirrors sets in on the periphery of the mirrors. It is obvious that with increasing pump the mode divergence of the resonator with the solid mirrors increases much more rapidly (multimode lasing) than the divergence of the lobes of the periodic modes (cf. Fig. 5, (2, 1), (2, 2), (2, 3)). The bright spot at the center is due to lasing on the periphery of the mirrors.

An important role in the shaping of narrow directivity patterns is played by the dependence of the field of the periodic modes on the porosity σ of the reticular mirror. With increasing σ , the envelope of b_n in (22) shrinks and at $\sigma \gg 1$ practically all the mode energy (~80%) should be concentrated in a single lobe for the mode with $n_0 = 0$ and $m_0 = 0$, in two lobes at $n_0 = 0, m_0 \neq 0$ or $n_0 \neq 0, m_0 = 0$, and in four at $n_0 \neq 0, m_0 \neq 0$.

The intensity distribution in the far zone at $\sigma = 50$, at a pump 15% above threshold, is shown in Fig. 6. The angle spectrum corresponds to excitation of one mode.

The angle divergence of the lobes of the periodic modes is apparently influenced by the nonmonochromaticity of the neodymium-laser emission and by the scattering of its optical inhomogeneities. The lobe width exceeds the diffraction value by several times and increases with increasing pump. In addition, a pedestal grows under the entire diagram. A similar situation obtains in lasers with stable resonators^[15] and is ascribed to scattering of the radiation as a result of thermo-optical distortions of the active medium.

We note that the wavelength dependence of the distance at which the periodic structure is reproduced makes it possible to tune the lasing frequency when the resonator length is varied.

CONCLUSION

The theoretical and experimental investigations show that a resonator with a mirror in the form of a two-di-

rectional grid with a period p has singular oscillation modes—periodic modes whose fields fill the entire exit aperture. At a resonator length L these modes will be oscillations with wavelengths that are multiples of $p^2/2L$.

Comparison of experiment with theory shows that the role of the finite dimensions of the mirrors is not so important. The field distribution and the spectral composition of the natural modes are determined with sufficient accuracy within the framework of the problem with infinite mirrors. A similar situation obtains in the case of reproduction of a passive grating.^[16]

The ORPB shapes a radiation directivity pattern that is determined by the parameters of the grid (dimension, period, porosity). The directivity pattern of a laser with an ORPB is of the many-lobe type, and the divergence of a single lobe should be determined by the diffraction by the total aperture. The ORPB make it possible to vary the character of the spatial distribution of the radiation and, in particular, make it possible to obtain extremely narrow single-lobe directivity patterns.

¹A. M. Prokhorov, *Zh. Eksp. Teor. Fiz.* **34**, 1658 (1958) [*Sov. Phys. JETP* **7**, 1140 (1958)].

²A. G. Fox and T. Li, *Bell Syst. Tech. J.* **40**, 453 (1961);

³L. A. Vainshtein, *Otkrytye rezonatory i otkrytye volnovody* (Open Resonators and Open Waveguides), Sovetskoe radio, 1966.

⁴E. A. Sziklas and A. E. Siegman, *Appl. Opt.* **14**, 1874 (1975).

⁵Yu. A. Anan'ev, N. A. Svetsitskaya, and V. E. Sherstobitov, *Zh. Eksp. Teor. Fiz.* **55**, 130 (1968) [*Sov. Phys. JETP* **28**, 69 (1969)].

⁶V. K. Ablekov, V. S. Belyaev, V. M. Marchenko, and A. M. Prokhorov, *Dokl. Akad. Nauk SSSR* **230**, 1066 (1976) [*Sov. Phys. Dokl.* **21**, 575 (1976)].

⁷Yu. V. Troitskiĭ, *Odnoshastotnaya generatsiya v gazovykh lazerakh* (Single-Frequency Generation in Gas Lasers), Nauka, Novosibirsk, 1975.

⁸Yu. A. Anan'ev, N. I. Grishmanova, and N. A. Svetsitskaya, *Zh. Tekh. Fiz.* **43**, 1530 (1973) [*Sov. Phys. Tech. Phys.* **18**, 968 (1974)].

⁹V. P. Shestopalov, *Difraktsionnaya elektronika* (Diffraction Electronics), Vysshaya shkola, Khar'kov, 1976.

¹⁰S. I. Averkov and N. I. Furashov, *Izv. Vyssh. Uchebn. Zaved. Radiofiz.* **12**, 1532 (1969).

¹¹V. V. Lyubimov, *Opt. Spektrosk.* **40**, 1080 (1976) [*Opt. Spectrosc. (USSR)* **40**, 622 (1976)].

¹²V. K. Ablekov and V. S. Belyaev, *Zh. Prikl. Spektrosk.* **23**, 1110 (1975).

¹³V. M. Marchenko, T. M. Makhviladze, A. M. Prokhorov, and M. E. Sarychev, *Preprint Fiz. Inst. Akad. Nauk No.* **20**, 1977.

¹⁴R. F. Edgar, *Opt. Acta* **16**, 281 (1969).

¹⁵Yu. A. Anan'ev, G. N. Vinokurov, L. V. Koval'chuk, N. A. Svetsitskaya, and V. E. Sherstobitov, *Zh. Ekspe. Teor. Fiz.* **58**, 786 (1970) [*Sov. Phys. JETP* **31**, 420 (1970)].

¹⁶Yu. N. Denis'yuk, N. M. Ramishvili, and V. V. Chavchanidze, *Opt. Spektrosk.* **30**, 1130 (1971).

Translated by J. G. Adashko